

Jelena T. Ilić
Assistant Professor
University of Belgrade
Faculty of Mechanical Engineering

Slavica S. Ristić
Principal Researcher fellow
Institute Goša, Belgrade

Dorđe S. Čantrak
Teaching Assistant
University of Belgrade
Faculty of Mechanical Engineering

Novica Z. Janković
Teaching Assistant
University of Belgrade
Faculty of Mechanical Engineering

Mileša Ž. Srećković
Full Professor
University of Belgrade
Faculty of Electrical Engineering

The Comparison of Air Flow LDA Measurement in Simple Cylindrical and Cylindrical Tube with Flat External Wall

The application of 2D laser Doppler anemometry systems is considered, in the case of fluid flow confined in simple cylindrical and in cylindrical tube with flat external surface of the wall. Geometric optics laws are applied to the central lines of laser beams. Measurement volume dislocations, calibration angles and distances of measurement volume centre from the photo-detector field of view centre are expressed. The expressions derived in this paper were applied to specific turbulent swirl flow in pipe. That revealed several advantages of use of a simple cylindrical tube over nowadays favored use of cylindrical tube with flat external surface. Those results suggest that current avoiding of laser Doppler anemometry measurements with simple cylindrical tubes should be reconsidered.

Keywords: laser Doppler anemometry, Snell's law, measurement volume dislocation, decalibration

1. INTRODUCTION

Fluid flow researchers warmly welcomed laser Doppler anemometry (LDA) as nonintrusive and absolute velocity measurement technique (requires no calibration) that has high temporal resolution, providing enough data to generate reliable statistics for local turbulences. Its development towards two and three velocity component measurements promised even better view of complex flows. All those benefits are thoroughly verified in the case of open fluid flows. Confined flows, however, apart from requiring transparent sections of vessels and tubes, suffered the refraction of both laser beams that produce measurement volume and scattered light that provides the velocity data. Any type of transparent wall, even the plan-parallel one, might generate some unwanted phenomena that must be taken into account: measurement volume dislocation, decalibration of a system, digression of measurement volumes for different velocity components (astigmatism), interference fringe distortion due to beam waist dislocation, etc. The degree of those unwanted phenomena depends on experimental settings and especially on its geometry.

As for cylindrical tube flows, among the first analytical approaches is one of Gardavsky et al. [1] that suggested the method of calculating the position of measurement volume and calibration angle along the diameter that overlaps the LDA system axis. Later, in order to minimize the wall curvature effects, flat external wall surfaces were applied [2-4]. Most of them considered liquid flows. More recently Zhang et al. performed several thorough analyses of the water flow within the tube of cylindrical internal and flat external wall [5,6]. Our attempts of experiments with LDA

application in air flows in simple cylindrical and in tube with cylindrical internal and flat external wall showed the severe problems, especially in the second configuration. That incited the detailed analysis exposed in this paper.

The propagation of LDA incident laser beams and scattered light, in the case of a simple cylindrical tube, are analysed by means of geometric optics in Section 2. The same but in a tube with cylindrical internal and flat external wall is analysed in Section 3. The intention is to measure the flow velocities along the diameter of a tube cross-section parallel to the lens, using two component LDA system.

Theoretical analysis of this paper explains how to find: 1. the dislocation of measurement volume in x and y direction Δx and Δy , respectively, as well as the resultant calibration angle in the measurement of radial (Sections 2.1 and 3.1), and axial (Sections 2.2 and 3.2) velocity components; 2. how far the measurement volume centre is from the centre of the field of view of the photo-detector of the LDA system, placed in the centre of the lens (the beginnings of Sections 2 and 3).

Optical aberrations, beam waist dislocations and fringe distortions were not taken into account and will be subject of further research. Still, the results of calculations according to the theory exposed in Sections 2 and 3 show several advantages of the use of simple cylindrical tubes over the use of flat external wall tube in the case of air flow (Section 4).

2. THE ANALYSIS IN A CASE OF A SIMPLE CYLINDRICAL TUBE

In turbulent swirl flow experiment that is the subject of this paper, the system enables only vertical traversing of a probe i.e. along the y axis (Fig. 1). There are two pairs of laser beams: one pair with vertical intersecting angle of 2θ (thick gray intersecting lines), measuring radial (vertical) velocity component v_r ; and another pair with horizontal intersecting angle of 2θ , too (thick gray dashed intersecting lines), that measures axial

Received: June 2012, Accepted: July 2013

Correspondence to: Jelena Ilić
Faculty of Mechanical Engineering,
Kraljice Marije 16, 11120 Belgrade 35, Serbia
E-mail: jilic@mas.bg.ac.rs

(horizontal) velocity component \vec{u} . The beam separation of both pairs of beams at lens is d :

$$d = 2f \tan \theta, \quad (1)$$

where f is the focal length of the lens.

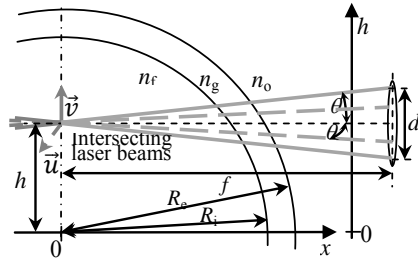


Figure 1. The definition of the geometry of a system with simple cylindrical tube

If there had not been a tube wall, the measurement volume would have been at focal length f distance from the lens (Fig. 1). However, due to refraction of laser beams on a tube wall, the dislocation of beam intersection point, i.e. measurement volume, appears.

It is supposed that the perfect transparent cylindrical tube, of internal radius R_i and external radius R_e , is horizontal, while lens is traversing in vertical direction. The lens position is defined by h which is the height of the lens centre with respect to the height of the centre of the tube cross-section (Fig. 1). The distance between the lens and the vertical diameter of the tube cross-section is supposed to be constant and equals the focal length f . Refraction indices of a fluid within a tube, tube glass, and external fluid are n_f , n_g and n_o , respectively. In this paper it is assumed that the refraction index of glass n_g is higher than refraction index of internal flowing fluid n_f , which is greater than or equal to that of external fluid (usually air) n_o .

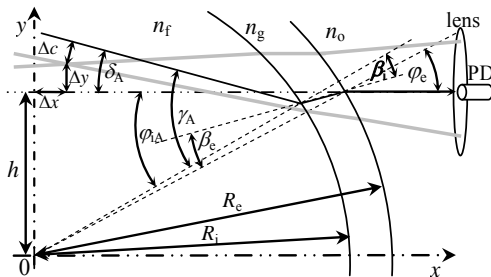


Figure 2. The path of the light that reaches the centre of the photo-detector through simple cylindrical tube wall

In Fig. 2, full black broken line presents the path of the light that reaches the centre of the photo-detector. It enters the photo-detector in the horizontal direction, but it does not come from the horizontal direction in the internal fluid, but at angle $\delta_A = \gamma_A - \varphi_{iA}$ to the horizontal where $\varphi_{iA} = \varphi_{eA} + \beta_{iA} - \beta_{eA}$ and

$$\begin{aligned} \sin \varphi_{eA} &= \frac{h}{R_e}, \quad \sin \gamma_A = \frac{n_0 h}{n_f R_i}, \\ \sin \beta_{eA} &= \frac{n_0 h}{n_g R_e}, \quad \sin \beta_{iA} = \frac{n_0 h}{n_g R_i} \end{aligned} \quad (2)$$

After calculating those angles and Δx and Δy , the distance of a centre of measurement volume from the centre of the viewing field of the photo-detector can be obtained as

$$\Delta c = R_i \sin(\varphi_{iA} + \delta_A) - \Delta x \sin \delta_A - (h + \Delta y) \cos \delta_A \quad (3)$$

2.1 Vertical LDA optical plane

Measurement volume dislocation is calculated according to Fig. 3. Each laser beam intersects the tube wall at two points: external (e) and internal (i). Higher beam intersects the external surface of the tube wall at point H_e , and the internal surface of the tube wall at point H_i . Lower beam intersects the external surface of the tube wall at point L_e , and the internal surface of the tube wall at point L_i . The positions of these four points with respect to the centre of the tube cross-section O and horizontal line (double dot – dash line) are defined by angles φ_{He} , φ_{Hi} , φ_{Le} and φ_{Li} , respectively.

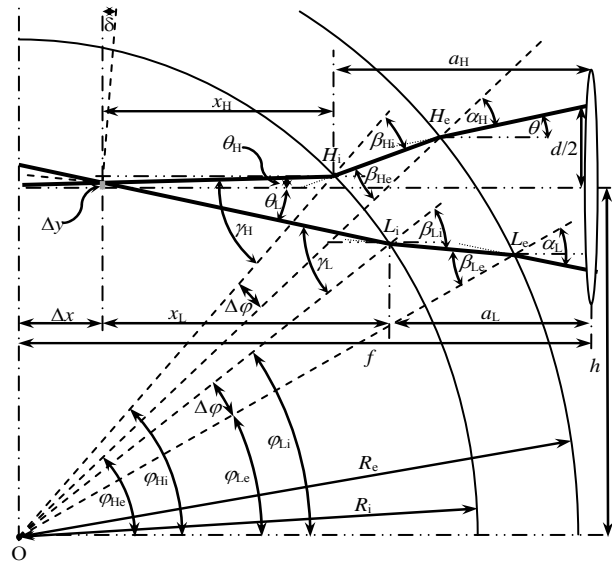


Figure 3. The propagation of LDA laser beams intersecting in vertical plane

In Fig. 3, it can be seen that:

$$R_e \sin \varphi_{(H/L)e} \pm (f - R_e \cos \varphi_{(H/L)e}) \tan \theta = h \quad (4)$$

With (1), by solving the (4), we obtain

$$\begin{aligned} \sin \varphi_{(H/L)e} &= \frac{h}{R_e} (\cos \theta)^2 \pm \\ &\pm \sin \theta \sqrt{1 - \left(\frac{h}{R_e}\right)^2 (\cos \theta)^2}, \end{aligned} \quad (5)$$

where sign + refers to φ_{He} , and sign - refers to φ_{Le} . The angles of incidence at glass surface of laser beams are

$$\alpha_{H/L} = \varphi_{(H/L)e} \mp \theta, \quad (6)$$

where - refers to α_{Hi} , and + refers to the α_{Li} . According to Snell's law, the angles of refraction at the external surface are $\sin \beta_{(H/L)e} = n_0 \sin(\varphi_{(H/L)e} \mp \theta) / n_g$. The law of sines applied to triangles OH_eH_i and OL_eL_i gives

$$\begin{aligned} \sin \beta_{(H/L)i} &= \frac{R_e \sin \beta_{(H/L)e}}{R_i} = \\ &= \frac{R_e n_0}{R_i n_g} \sin(\varphi_{(H/L)e} \mp \theta) \end{aligned} \quad (7)$$

which defines angles of incidence of beams at the internal tube surface (Fig. 3). Snell's law applied at that surface and (7) lead to internal angles of refraction $\gamma_{H/L}$

$$\sin \gamma_{H/L} = \frac{n_0}{n_f} \frac{R_e}{R_i} \sin(\varphi_{(H/L)e} \mp \theta). \quad (8)$$

Laser beams in fluid (within the tube) are inclined to the horizontal (double dot – dash) lines at angles

$$\theta_H = \varphi_{Hi} - \gamma_H \text{ and } \theta_L = \gamma_L - \varphi_{Li}, \quad (9)$$

(θ_H is the angle between the higher beam and the horizontal line, and θ_L is the angle between the lower beam and the horizontal line in the internal fluid). Fig. 3 shows that $\beta_{(H/L)i} = \beta_{(H/L)e} + \Delta\varphi_{H/L}$ ($\Delta\varphi_{H/L} = \Delta\varphi_{(H/L)i} - \Delta\varphi_{(H/L)e}$).

The resultant beam intersection angle, which defines calibration constant of a system, is

$$\begin{aligned} \theta_r &= \frac{\theta_H + \theta_L}{2} = \\ &= \frac{1}{2}(\Delta\varphi_e + \Delta\beta_i - \Delta\beta_e - \Delta\gamma) \end{aligned} \quad (10)$$

where $\Delta\varphi_e = \Delta\varphi_{He} - \Delta\varphi_{Le}$, $\Delta\beta_i = \beta_{Hi} - \beta_{Li}$, $\Delta\beta_e = \beta_{He} - \beta_{Le}$ and $\Delta\gamma = \gamma_H - \gamma_L$.

Since the bisector of the beam intersection angle is no more horizontal, measured velocity component inclines to the vertical axes at angle

$$\delta = (\theta_H - \theta_L)/2. \quad (11)$$

Between the lens and intersecting point, each beam is broken into three line segments, due to refraction: the first in external fluid, the second in glass, and the third in internal flowing fluid. It can be noted that the sum of the projections of those three line segments upon a horizontal line for one laser beam is equal to that of another laser beam i.e.

$$x_H + a_H = x_L + a_L. \quad (12)$$

x_H is horizontal distance between H_i and the actual beam intersection point, and x_L is horizontal distance between L_i and actual beam intersection point (Fig. 3). a_H is horizontal distance between lens and H_i , and a_L is horizontal distance between lens and L_i . They can be expressed as

$$\begin{aligned} a_H &= |H_i H_e| \cos(\varphi_{Hi} - \beta_{Hi}) + \\ &+ (f - R_e \cos \varphi_{He}) \\ a_L &= |L_i L_e| \cos(\beta_{Li} - \varphi_{Li}) + \\ &+ (f - R_e \cos \varphi_{Le}) \end{aligned} \quad (13)$$

where

$$\begin{aligned} |H_i H_e| &= \\ &= \sqrt{R_e^2 + R_i^2 - 2R_e R_i \cos(\varphi_{Hi} - \varphi_{He})} \end{aligned} \quad (13a)$$

$$\begin{aligned} |L_i L_e| &= \\ &= \sqrt{R_e^2 + R_i^2 - 2R_e R_i \cos(\varphi_{Li} - \varphi_{Le})} \end{aligned} \quad (13b)$$

Also, the sum of the projections of those three line segments upon a vertical line for one laser beam plus that of another laser beam equals beam separation at the lens d i.e.

$$x_H \tan \theta_H + b_H + x_L \tan \theta_L + b_L = d. \quad (14)$$

b_H is vertical distance between the position of higher beam at lens and H_i , and b_L is vertical distance between the position of lower beam at lens and L_i . They can be expressed as

$$\begin{aligned} b_H &= |H_i H_e| \sin(\varphi_{Hi} - \beta_{Hi}) + \\ &+ (f - R_e \cos \varphi_{He}) \tan \theta \\ b_L &= |L_i L_e| \sin(\beta_{Li} - \varphi_{Li}) + \\ &+ (f - R_e \cos \varphi_{Le}) \tan \theta \end{aligned} \quad (15)$$

Finding x_H and x_L from the system (12) and (14), enables calculating the horizontal and vertical displacement of measurement volume Δx and Δy , respectively (Fig. 3):

$$\Delta x = f - x_H - a_H$$

and

$$\Delta y = f \tan \theta - x_H \tan \theta_H - b_H. \quad (16)$$

2.2 Horizontal LDA optical plane

In this case laser beams are in horizontal plane between the lens and the tube wall. Unlike the previous case, where both laser beams and all their segments were in the same plane – vertical plane, here the refractions on each side of the tube wall force laser beams to change the plane in which they propagate. The symmetry of considered geometry allows analysing the refraction of only one laser beam, because another beam undergoes exactly the same changes until the point of intersection.

The first task is to find out the angle of incidence of a laser beam (thick grey line) at the external surface of a tube – angle α . Laser beam reaches the external surface of a tube at point E (Fig. 4). The angle φ_e between the ray OE and horizontal lines (double dot – dash lines) is related to the height of the centre of a lens h as follows:

$$\sin \varphi_e = h/R_e. \quad (17)$$

The plane ABC perpendicular to the laser beam at point A , helps in finding the angle α . Noting the right angles in Fig. 4, it can be concluded that

$$\cos \alpha = \cos \varphi_e \cos \theta. \quad (18)$$

The angle of incidence α lies in plane ACE which is inclined to the horizontal plane ABE at angle γ . Among other expressions for angle γ , one that avoids sign ambiguity and division by zero, is following expression:

$$\tan \gamma = \frac{\tan \varphi_g}{\sin \theta} \quad (19)$$

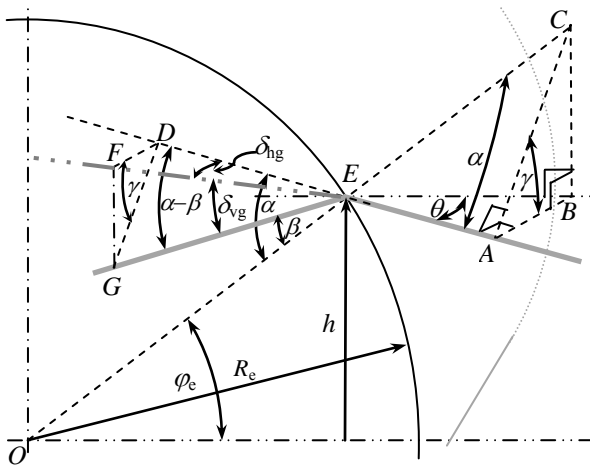


Figure 4. The incidence of a laser beam at the external surface of a tube wall and the propagation direction of a laser beam (thick grey line) within the glass of a tube wall

Applying the Snell's law, the angle β at which laser beam enters the glass is determined as $\sin \beta = n_0 \sin \alpha / n_g$.

Angle β belongs to the plane ACE which can also be designated as plane EDG , as well (Fig. 4). The projection of refracted laser beam upon horizontal plane EDF (or ABE) is ray EF presented as grey double dot – dash line. Its deviation from the initial direction of laser beam (i.e. ray ED) is angle δ_{hg} , and its deviation from the direction of refracted laser beam (i.e. ray EG) is angle δ_{vg} . In order to express angles δ_{hg} and δ_{vg} , plane DFG parallel to the plane ABC should be noted. The analysis of a tetrahedron $EDFG$ shows that

$$\begin{aligned} \sin \delta_{vg} &= \sin(\alpha - \beta) \sin \gamma & \text{and} \\ \cos \delta_{hg} &= \cos(\alpha - \beta) / \cos \delta_{vg} \end{aligned} \quad (20)$$

Again, exactly the same changes undergoes the other beam but at the opposite side with respect to the plane perpendicular to the tube axis. Therefore, entering the glass, laser beams propagate in plane EHG which is inclined at angle δ_{rg} to the horizontal plane (plane EHF – Fig. 5).

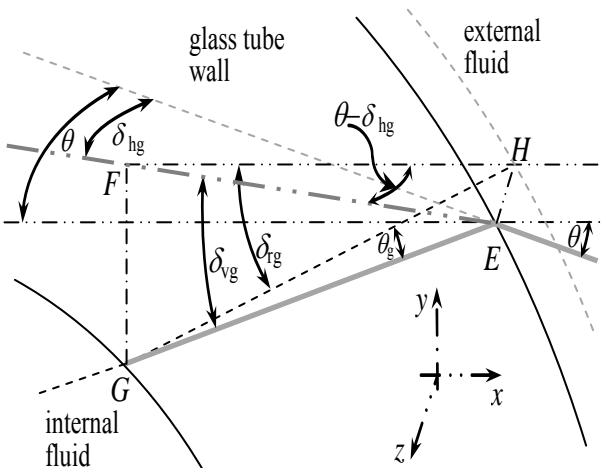


Figure 5. The spatial position of a laser beam GE within the glass of a tube wall

Note that triangles EFG and HFG are right angled triangles with right angle at point F , and triangles EHG and EHF are right angled triangles with right angle at point H . It helps in expressing angle δ_{rg} as

$$\tan \delta_{rg} = \frac{\tan \delta_{vg}}{\cos(\theta - \delta_{hg})} \quad (21)$$

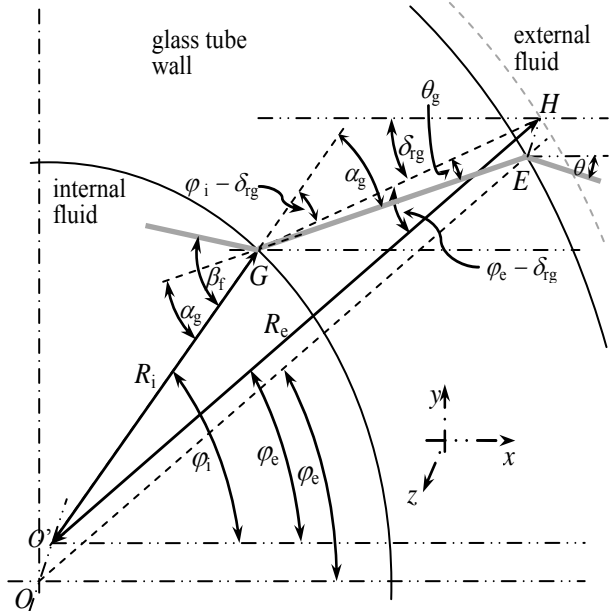


Figure 6. The incidence of a laser beam at the internal surface of a tube wall

If laser beams have been intersecting within the glass, they would intersect at angle θ_g (Figs. 5, 6), which can be expressed as

$$\sin \theta_g = \cos \delta_{vg} \sin(\theta - \delta_{hg}) \quad (22)$$

At point G , the laser beam reaches the internal surface of a tube wall, and suffers another refraction. In order to find the angle of incidence at point G , the angle φ_i , defining its position with respect to the centre of a tube cross – section and horizontal line, should be discovered (Fig. 6). (While point E belongs to the cross – section with centre in point O , points H and G belong to the cross-section with centre in point O' shifted along the tube axis OO' for the same length as it is the length of line segment EH .) Applying the law of sines to the triangle $O'HG$, we obtain

$$\varphi_i = \delta_{rg} + \sin^{-1} \left(\frac{R_e}{R_i} \sin(\varphi_e - \delta_{rg}) \right) \quad (23)$$

The angle of incidence α_g can be found in a way similar to that in the case of the incidence of laser beam at the external surface of a tube wall – instead of φ_e , here it is $\varphi_i - \delta_{rg}$, and instead of θ , here it is θ_g :

$$\cos \alpha_g = \cos(\varphi_i - \delta_{rg}) \cos \theta_g \quad (24)$$

Applying the Snell's law, the angle of refraction in the internal fluid β_f is obtained as $\sin \beta_f = n_g \sin \alpha_g / n_f$.

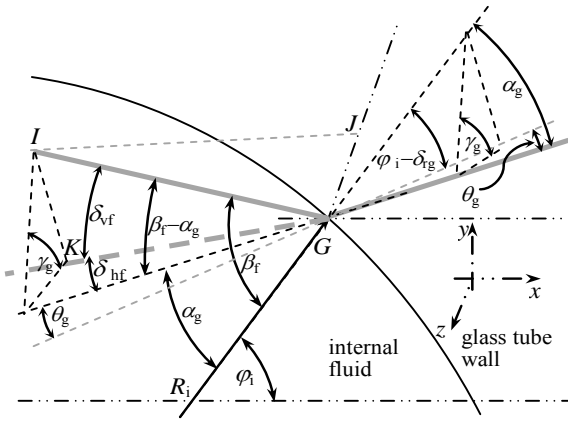


Figure 7. The refraction of a laser beam at the internal surface of a tube wall

To get better view at propagation of the laser beam after the second refraction, Fig. 7 could be useful. Note that it resembles Fig. 4: as if all rays emerging from point *E* were translated to the point *G* and then rotated around the horizontal *GJ* (parallel to the tube axis) counter clockwise for angle δ_{rg} . That is why the expressions for angles in Fig. 7 resemble the expressions for angles in Fig. 4. The difference is in a fact that here refracted laser beam goes above the plane of angle θ_g ($n_g > n_r$), while in previous refraction refracted beam went under the plane of angle θ_g ($n_g > n_o$). Thus the angle between the plane containing angle α_g and the plane containing angle θ_g is angle γ_g that could be expressed as

$$\tan \gamma_g = \frac{\tan(\varphi_i - \delta_{rg})}{\sin \theta_g} \quad (25)$$

The projection of refracted laser beam upon the plane that contains angle θ_g is ray *GK* presented as grey dashed line. Its deviation from the direction of laser beam in glass tube wall (i.e. ray *EG*) is angle δ_{hf} , and its deviation from the direction of refracted laser beam (i.e. ray *GI*) is angle δ_{vf} . Those angles could be expressed as

$$\begin{aligned} \sin \delta_{vf} &= \sin(\beta_f - \alpha_g) \sin \gamma_g, & \text{and} \\ \cos \delta_{hf} &= \frac{\cos(\beta_f - \alpha_g)}{\cos \delta_{vf}} \end{aligned} \quad (26)$$

Triangles *KGI* and *KJI* (Fig. 8) are right angled triangles with right angle at point *K*, and triangles *KGJ* and *IGJ* are right angled triangles with right angle at point *J*. Therefore, in the internal fluid, laser beam propagates in the plane *IGJ*, that is inclined to the plane of incidence at point *G* at angle δ_{rf} which can be expressed as

$$\tan \delta_{rf} = \frac{\tan \delta_{vf}}{\sin(\theta_g + \delta_{hf})} \quad (27)$$

The analysis of same triangles leads to the resultant half-angle of laser beam intersection θ_r – the angle that defines the calibration constant of the LDA system:

$$\sin \theta_r = \cos \delta_{vf} \sin(\theta_g + \delta_{hf}) \quad (28)$$

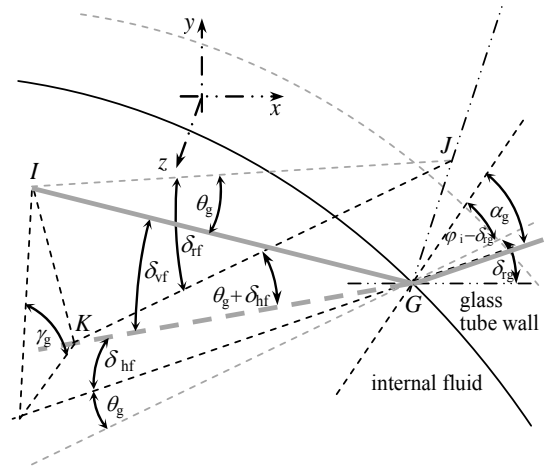


Figure 8. The spatial position of a laser beam in the internal fluid

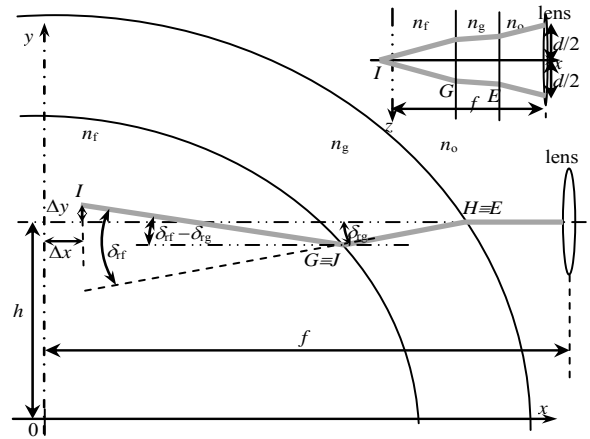


Figure 9. Frontal view of laser beams (big picture) and view from above (small picture at the right up)

In order to find the dislocation of measurement volume the lengths of line segments *GH* and *IJ* are required. The length of line segment *GH* could be found by applying the law of cosines to the triangle *O'HG*, as follows

$$|GH| = \sqrt{R_e^2 + R_i^2 - 2R_e R_i \cos(\varphi_i - \varphi_e)} \quad (29)$$

Observing the Figs. 5 and 8, it can be concluded that

$$|IJ| \tan \theta_r + |GH| \tan \theta_g = R_e \cos \varphi_e \tan \theta \quad (30)$$

It gives the length of line segment *IJ*.

Finally, analysing the frontal view of a system (Fig. 9) the dislocations of measurement volume centre in *x* and *y* direction can be expressed as

$$\begin{aligned} \Delta x &= R_e \cos \varphi_e - |GH| \cos \delta_{rg} - |IJ| \cos(\delta_{rf} - \delta_{rg}) \\ \Delta y &= |IJ| \sin(\delta_{rf} - \delta_{rg}) - |GH| \sin \delta_{rg} \end{aligned} \quad (31)$$

Unlike the case of vertical laser beam intersecting angle, here the direction of measured velocity component does not change – axial velocity component is measured, always.

3. THE CASE OF A CYLINDRICAL INTERNAL AND FLAT EXTERNAL TUBE WALL

Frequently used way of LDA measurement is presented in Fig. 10. The internal surface of a tube is cylindrical with radius of cross-section R , but external surface of a tube wall is flat, at least at the side that faces the lens. The least thickness of wall is d_w . Again, the pair of laser beams, whose intersecting angle 2θ is vertical, is presented by full thick grey line, and that, whose intersecting angle 2θ is horizontal, is presented by dashed thick grey line. The real refraction of laser beams is not presented in Fig. 10 due to complexity.

Three chosen horizontal positions of lens are considered: Case 1 when the distance between the lens and the external tube wall is $l = f - (R + d_w)$; Case 2 when vertical pair of laser beams intersects in the centre of a circular cross section (as in Fig. 10), and the distance between the lens and the external surface of a tube l is

$$l = f - (R + d_w) \frac{\tan \theta_g}{\tan \theta}, \quad (32)$$

where θ_g is the angle of refraction in glass that can be expressed as $\sin \theta_g = n_o \sin \theta / n_g$; and Case 3 when horizontal pair of laser beams intersects at the centre of a circular cross-section, and l is

$$l = f - R \frac{\tan(\sin^{-1}(n_g \sin \theta_g / n_f))}{\tan \theta} - d_w \frac{\tan \theta_g}{\tan \theta}. \quad (33)$$

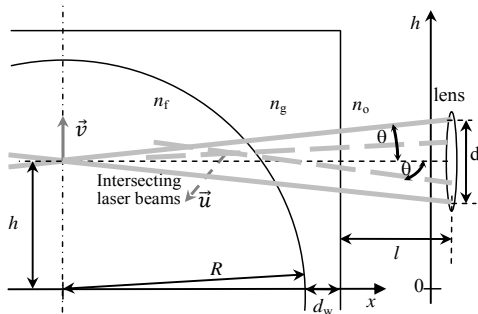


Figure 10. The definition of the geometry of a system with cylindrical tube having flat external surface of the wall

For flat external wall, the distance of the centre of the measurement volume from the centre of the viewing field of a photo-detector should be calculated, too.

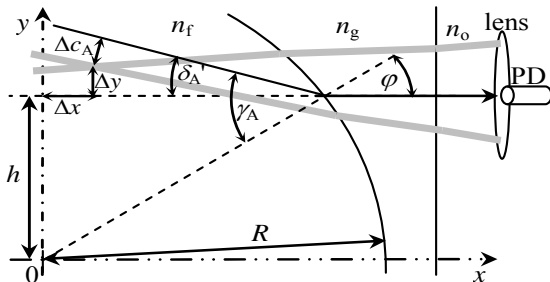


Figure 11. The path of the light that reaches the centre of the photo-detector through tube wall with flat external wall

Inside the tube (Fig. 11), the path of the light that reaches the centre of the photo-detector is inclined to the horizontal at angle $\delta_A = \gamma_A - \varphi$, where

$$\sin \varphi = \frac{h}{R} \quad \text{and} \quad \sin \gamma_A = \frac{n_g h}{n_f R}. \quad (34)$$

With this and Δx and Δy calculated, the distance between the centre of the measurement volume and the centre of the viewing field is

$$\Delta c_A = (R_i \cos \varphi - \Delta x) \sin \delta_A - \Delta y \cos \delta_A \quad (35)$$

3.1 Vertical LDA optical plane

After the refraction of laser beams at the external surface of a glass tube, they reach the internal surface of a tube at points that can be defined by φ_H for higher, and φ_L for lower laser beam. Those angles can be found as

$$\sin \varphi_{H/L} = t_{H/L} (\cos \theta_g)^2 \pm \sin \theta_g \sqrt{1 - t_{H/L}^2 (\cos \theta_g)^2}, \quad (36)$$

where sign + refers to the higher, sign - refers to the lower beam, and parameter t_H and t_L are $t_{H/L} = (h \pm t_1) / R$.

Again, sign + refers to the higher, sign - refers to the lower beam, and parameter t_1 is

$$t_1 = d/2 - (l \tan \theta + R_e \tan \theta_g). \quad (37)$$

Then, laser beams refract at the internal surface of a glass tube with the angle of refraction, defined as $\sin \beta_{H/L} = n_g \sin(\varphi_{H/L} \mp \theta_g) / n_f$. Now, sign - refers to the higher, sign + refers to the lower beam. After that refraction, the directions of higher and lower laser beam, with respect to the horizontal lines, are at angles

$$\theta_H = \varphi_H - \beta_H \quad \text{and} \quad \theta_L = \beta_L - \varphi_L \quad (38)$$

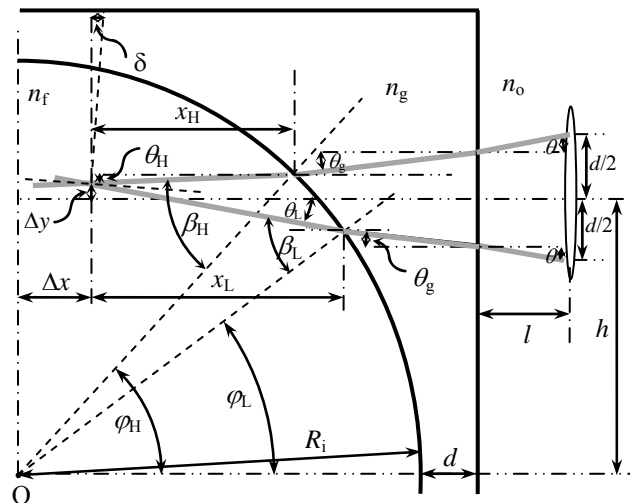


Figure 12. The propagation of laser beams in the case of vertical LDA optical plane and flat external wall of a tube

The horizontal distances between the point of intersection of the beams and points at which beams

reach the internal surface of a tube are x_L for lower, and x_H for higher beam (Fig. 12). They can be expressed as

$$x_L = \frac{t_2 \tan \theta_H + t_3}{\tan \theta_H + \tan \theta_L} \text{ and } x_H = x_L - t_2, \quad (39)$$

where parameters t_2 and t_3 are

$$t_2 = R(\cos \varphi_L - \cos \varphi_H), \quad (40)$$

and

$$t_3 = 2t_1 + R(\cos \varphi_L + \cos \varphi_H) \tan \theta_g. \quad (41)$$

The dislocations of measurement volume x and y directions are

$$\Delta x = R \cos \varphi_H - x_H \text{ and} \\ \Delta y = R \sin \varphi_H - x_H \tan \theta_H - h \quad (42)$$

3.2 Horizontal LDA optical plane

Laser beams paths are symmetrical with respect to the vertical plane normal to the tube axis. Therefore, it is enough to consider the propagation of only one beam e.g. the one closer to the viewing point. First, this beam refracts at the external fluid –glass interface. Both, the angle of incidence θ and the angle of refraction θ_g (defined by Snell's law) are in horizontal plane. Then the beam reaches the internal surface of a tube at point A. Its position with respect to the centre of the tube cross-section and horizontal line φ is defined by $\sin \varphi = h/R$. The angle of incidence at point A is α (Fig. 13), and it can be expressed as

$$\cos \alpha = \cos \varphi \cos \theta_g. \quad (43)$$

Angle α lies in the plane AIC that is inclined to the horizontal plane at angle γ for which it stands that

$$\tan \gamma = \frac{\tan \varphi}{\sin \theta_g}. \quad (44)$$

The angle of refraction at point A is β determined as

$$\sin \beta = \frac{n_g \sin \alpha}{n_0}. \quad (45)$$

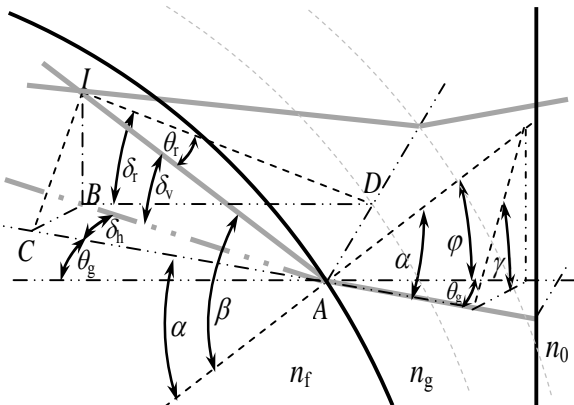


Figure 13. The propagation of laser beams in the case of vertical LDA optical plane and flat external wall of a tube

Observed laser beam propagates in the internal fluid along the ray AI. Its projection on a horizontal plane is ray AB, whose deviation from ray AI is angle δ_v , and deviation from ray AC is δ_h , defined as

$$\sin \delta_v = \sin(\beta - \alpha) \sin \gamma \text{ and} \\ \cos \delta_h = \cos(\beta - \alpha) / \cos \delta_v, \quad (46)$$

The projection of angle δ_v on the tube cross-section plane is angle δ_r that presents resultant deviation of laser beam from the horizontal in the fluid, and it can be expressed as

$$\tan \delta_r = \frac{\tan \delta_v}{\cos(\theta_g + \delta_h)}. \quad (47)$$

The resultant calibration angle θ_r (i.e. half of the angle of intersection of laser beams) is defined by

$$\sin \theta_r = \cos \delta_v \sin(\theta_g + \delta_h). \quad (48)$$

The horizontal penetration of the laser beam until the intersecting point I is

$$x = |DE| = \frac{t_1 + R_i \cos \varphi \tan \theta_g}{\tan(\theta_g + \delta_h)} \quad (49)$$

Finally, the distance of measurement volume from the vertical diameter of circular cross-section of a tube Δx , and from the horizontal $y=h$ are

$$\Delta x = R_i \cos \varphi - x \text{ and} \\ \Delta y = x \tan \delta_r \quad (50)$$

4. RESULTS AND DISCUSSION

The calculations explained in previous section are applied to the case of already performed LDA measurements with two component system (red $\lambda_1=660\text{nm}$ and infrared $\lambda_2=785\text{nm}$). External fluid as well as internal fluid is air ($n_0=n_f=1$). The tube is made of acrylic glass. The indices of refraction of tube wall glass are $n_g=1.4878$ for red light and $n_g=1.48452$ for infrared (IR) light [7]. The focal length of applied transmitting lens is $f=0.3\text{m}$, and the beam separation in the lens is $d=0.06\text{m}$. Thus, the calibration angle of this system in open air is $\theta=5.7106^\circ$. Measurement volume in open air is $1.267 \times 0.127 \times 0.121\text{mm}$ for red light, and $1.507 \times 0.1507 \times 0.1499\text{mm}$ for infrared light. Therefore, approximate diameter of viewing field of the photo-detector is supposed to be 0.121mm for red, and 0.1499mm for infra red light. Internal radius of a tube is $R_i=R=0.2\text{m}$ and external radius is $R_e=0.2055\text{m}$. In the case of flat external wall, the least wall thickness is $d_w=11\text{mm}$ (Fig. 10).

The influence of the thickness of the wall on LDA measurement could be analyzed in further research. The discussion and conclusions in this paper refer to the thicknesses and materials mentioned in previous paragraph. Performed calculations indicated at least five advantages of measurement with simple cylindrical tube over the measurement with the flat external wall tube.

1. In the case of simple cylindrical tube, calibration angle θ_r , is constant and the same as one in the open air (Table 1, the first data column). This means that, in this case, no corrections of the values of measured velocities are required. On the other hand, calibration angle, in the case of flat external wall, is smaller than that in the open air (which, among other issues, makes the measurement volume shorter), and the decalibration must be taken into account. In the case of radial velocity component measurement at lens positions 1 and 3 it is even not constant (Fig. 14). The change of the calibration angle presented in Fig. 14 is for infrared beams and it is almost the same in the case of infrared beams.

2. Measurement range, the range for which the measurement system gives any result, is shown in the second data column of Table 1. It is restricted by three phenomena: total reflection at the glass - internal fluid interface, laser beam intersection is outside the internal fluid and measurement volume is outside the viewing field of photo-detector. For simple cylindrical tube, measurement range encompasses almost the entire diameter (0-0.99R), whereas in Cases 1, 2 and 3, they are considerably smaller. In Case 1, when the distance between the lens and vertical diameter of the circular cross-section is f , vertical pair of laser beams does not intersect inside the tube at all.

3. The linearity of relation between the relative heights of lens centre h/R_i and measurement volume height $(h+\Delta y)/R_i$, is analyzed through the slope of linear regression a and its relative standard uncertainty u_{rel} – type A (last two data columns in Table 1). The slopes for simple cylindrical tube are close to 1, which means that vertical displacements of lens approximately equal the displacements of measurement volumes. The same does not stand for the flat external wall tube. Though the analysed regressions are very close to linear, values of u_{rel} show that the linearity of measurement with simple cylindrical tube is better than that for flat external wall for one order of magnitude in the case of axial velocity measurement, and for two orders of magnitudes in the case of radial velocity component measurement.

Table 1. The comparison of measurement in simple cylindrical and flat external – cylindrical internal wall tube

Tube type	Measured velocity component	Calibration angle θ_r (o)	Measure-ment range	Linearity	
				Slope a	u_{rel} (%)
Simple cylindrical	Red/IR Radial	5.7106	0-0.99R _i	0.999	0.073
	Red/IR Axial	5.7106	0-0.99R _i	1.001	0.079
Cylindrical internal and flat external surface	1 Radial	Fig. 14	0-0R	-	-
	1 Red/IR Axial	5.7098/5.6972	0-0.22R/0-0.26R	1.50	0.15/0.25
	2 Red/IR Radial	3.835/3.843	0-0.81R	1.4	3.34/3.43
	2 Red/IR Axial	5.7098/5.6972	0-0.28R/0-0.35R	1.33	0.13/0.17
	3 Red/IR Radial	Fig. 14	0-0.81R/0-0.86R	2.02/2.05	2.10/2.36
	3 Red/IR Axial	5.7098/5.6972	0-0.22R/0-0.27R	1.49	0.15/0.21

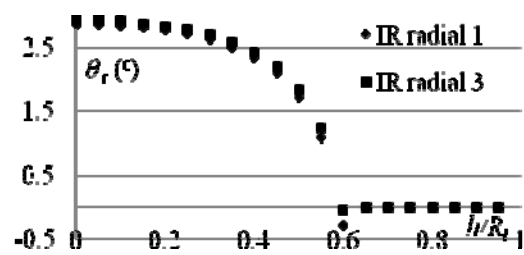


Figure 14. Calibration angle θ_r – the resultant half angle of the intersection of beams – versus vertical relative position of transmitting lens for the case of infrared laser beams and horizontal positions 1 and 3 for flat external tube wall

4. The dislocation of measurement volume from the desired points along the vertical diameter of a tube cross-section and mutual measurement volume distances can be seen in Figs. 15 -17. In Figs. 16 and 17, crosses represent positions of measurement volumes for axial velocity component in lens positions 2 and 3, but squares represent only those of them that are within the viewing field of photo-detector. Thus, for flat external tube wall and horizontal positions 2 and 3, the measurement volumes for the two components are simultaneously visible only within the central 25% of internal radius R_i . Furthermore, the measurement volume distances are greater than 0.3R for Case 2 and greater than 0.9R for Case 3. With simple cylindrical tube, for h up to 0.99R, measurement volumes for different velocity components are simultaneously visible in photo-detector. They are no more than 0.01R apart in half of the radius closer to tube centre, and rises only up to 0.055R near the tube wall. Smaller mutual distances of measurement volumes for different velocity components might also indicate smaller optical aberration of the beams in simple cylindrical tube.

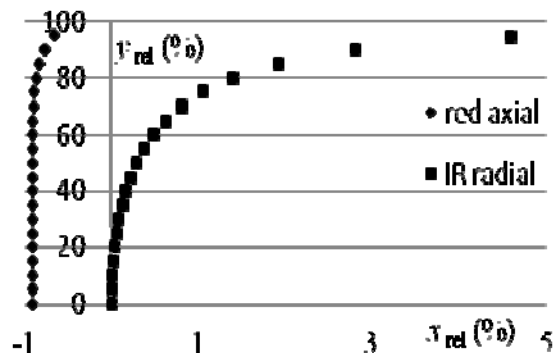


Figure 15. Simple cylindrical tube: Positions of IR measurement volume for radial velocity component, and red measurement volume for axial velocity component

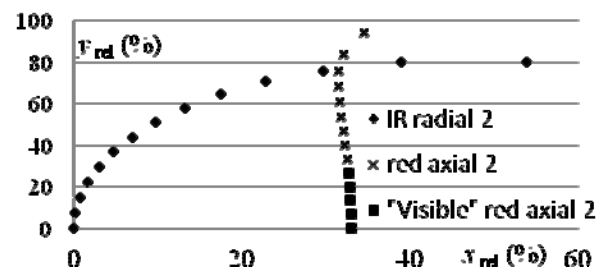


Figure 16. Cylindrical tube with flat external wall: Positions of IR measurement volume for radial velocity component, and red measurement volume for axial velocity component at position 2

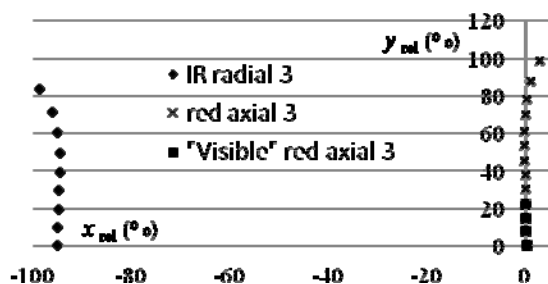


Figure 17. Cylindrical tube with flat external wall: Positions of IR measurement volume for radial velocity component and red measurement volume for axial velocity component at position 3

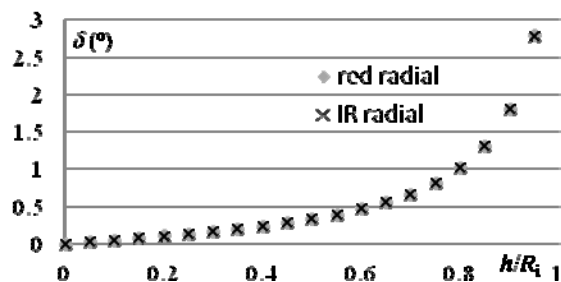


Figure 18. The angle of deviation of direction of measured radial velocity component, in simple cylindrical tube

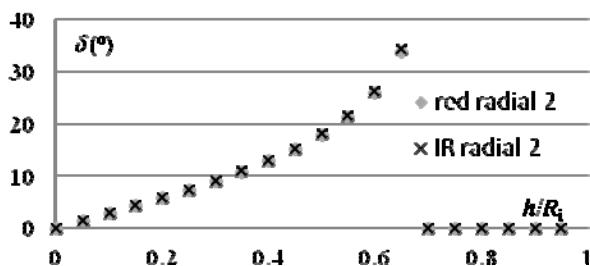


Figure 19. The angle of deviation of direction of measured radial velocity component, in a tube with flat external wall

5. In order to measure radial velocity component along the vertical diameter of a tube cross section, the bisector of beam intersecting angle must be horizontal. Its deviation from horizontal δ in simple cylindrical tube (Fig. 18) is negligible with respect to that in flat external wall tube (Fig. 19).

ACKNOWLEDGMENT

This paper is part of the research project TR35046 supported by the Ministry of Education and Science of the Republic of Serbia.

REFERENCES

[1] Gardavsky, J. and Hrbek, J.: Refraction corrections for LDA measurements in circular tubes within rectangular optical boxes, Dantec Information, No.8, pp.2-5, 1989.

[2] Wang, M.H., Bara, B., Hackman, L., Czarnecki, J., Afacan, A., Nandakumar, K. and Masliyah, J.H.: Hydrodynamics in gravity settling vessel: CFD modelling with LDA validation, The Canadian Journal of Chemical Engineering, Vol.78, pp.1046-1054, 2000.

[3] Castrejoin-Pita, J.R., del Rio, J.A., Castrejoin-Pita, A.A. and Huelsz, G.: Experimental observation of dramatic differences in the dynamic response of Newtonian and Maxwellian fluids, Physical Review E, Vol. 68, pp. 1-5, 2003.

[4] Otute, A. and Armenante, P.M.: Experimentally-validated micro-mixing-based CFD model for fed-batch stirred-tank reactors, AIChE Journal, Vol.50, No.3, pp.566-576, 2004.

[5] Zhang, Zh.: Optical guidelines and signal quality for LDA applications in circular pipes, Experiments in Fluids, Vol. 37, pp. 29-39, 2004.

[6] Zhang, Zh.: Rotating stall mechanism and stability control in the pump flows, IOP Conf. Series: Earth and Environmental Science 12, 012010, 2010.

[7] Kasarova, S.N., Sultanova, N.G., Ivanov, C.D. and Nikolov, I.D: Analysis of the dispersion of optical plastic materials, Optical Materials., Vol. 29, pp. 1481-1490, 2007.

ПОРЕЂЕЊЕ ЛДА МЕРЕЊА КОД ВАЗДУШНОГ ТОКА У ОБИЧНОЈ ЦИЛИНДРИЧНОЈ И ЦИЛИНДРИЧНОЈ ЦЕВИ СА РАВНИМ СПОЉАШЊИМ ЗИДОМ

Јелена Т. Илић, Славица С. Ристић, Ђорђе С. Чантрак, Новица З. Јанковић, Милеса Ж. Срећковић

Примена 2D ласер Доплер анемометарских система је разматрана за случај затвореног тока флуида у обичној цилиндричној и у цилиндричној цеви са равним спољашњим зидом. Закони геометријске оптике су примењени на централне линије ласерских снопова. Изведени су изрази за дислокације мерних запремина, углове калибрације и растојања центра мерне запремине од центра видног поља фотодетектора. Изрази изведени у овом раду су преименовани на одређени вртложни ток у цеви. То је показало неколико предности коришћења обичне цилиндричне цеви у односу на данас омиљеније коришћење цилиндричне цеви са равним спољашњим зидом. Ови резултати указују на то да би се садашње избегавање ЛДА мерења код обичне цилиндричне цеви требало преиспитати.